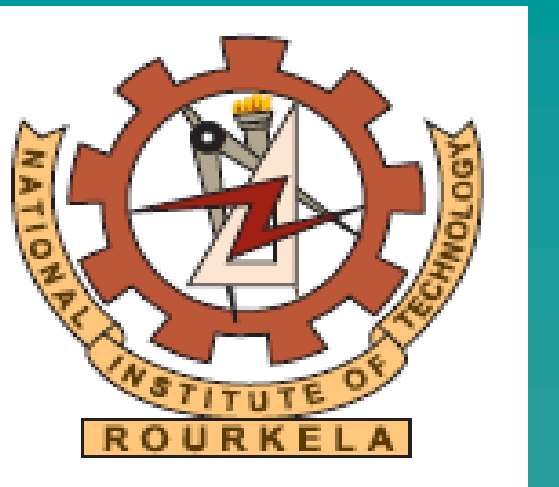


Stress-induced roller coaster model of autophagy leads to autophagic cell death

Sujit K. Bhutia*, Subhadip Mukhopadhyay

Department of Life sciences, National Institute of Technology Rourkela, India



Autophagy can either be cytoprotective or promote cell death in a context-dependent manner in response to stress. How autophagy leads to autophagic cell death requires further clarification. In this study, we document a nonlinear roller coaster form of autophagy oscillation when cells are subjected to different stress conditions. Serum starvation induces an initial primary autophagic peak at 6 h that is sufficient to reduce autophagy at 24 h by replenishing cells with de novo fluxed nutrients, but protracted stress leads to a secondary autophagic peak around 48 h. Time kinetic studies indicate that the primary autophagic peak is reversible, whereas the secondary autophagic peak is irreversible and leads to cell death. Key players involved in different stages of autophagy including initiation, elongation and degradation during this oscillatory sequence were identified. A similar molecular pattern was intensified under apoptosis-deficient conditions. mTOR was the central molecule regulating this autophagic activity, and upon knockdown a steady increase of autophagy without any non-linear fluctuation was evident. An unbiased proteome screening approach was employed to identify the autophagy molecules potentially regulating these autophagic peaks. Annexin A2 was identified as a unique stress-induced protein involved in modulating the point of irreversible autophagy leading to cell death through interaction with mTOR and altering its spatiotemporal cellular localization.

RESULTS

1. Cells under stress display a roller coaster form of non-linear, dynamic autophagy progression

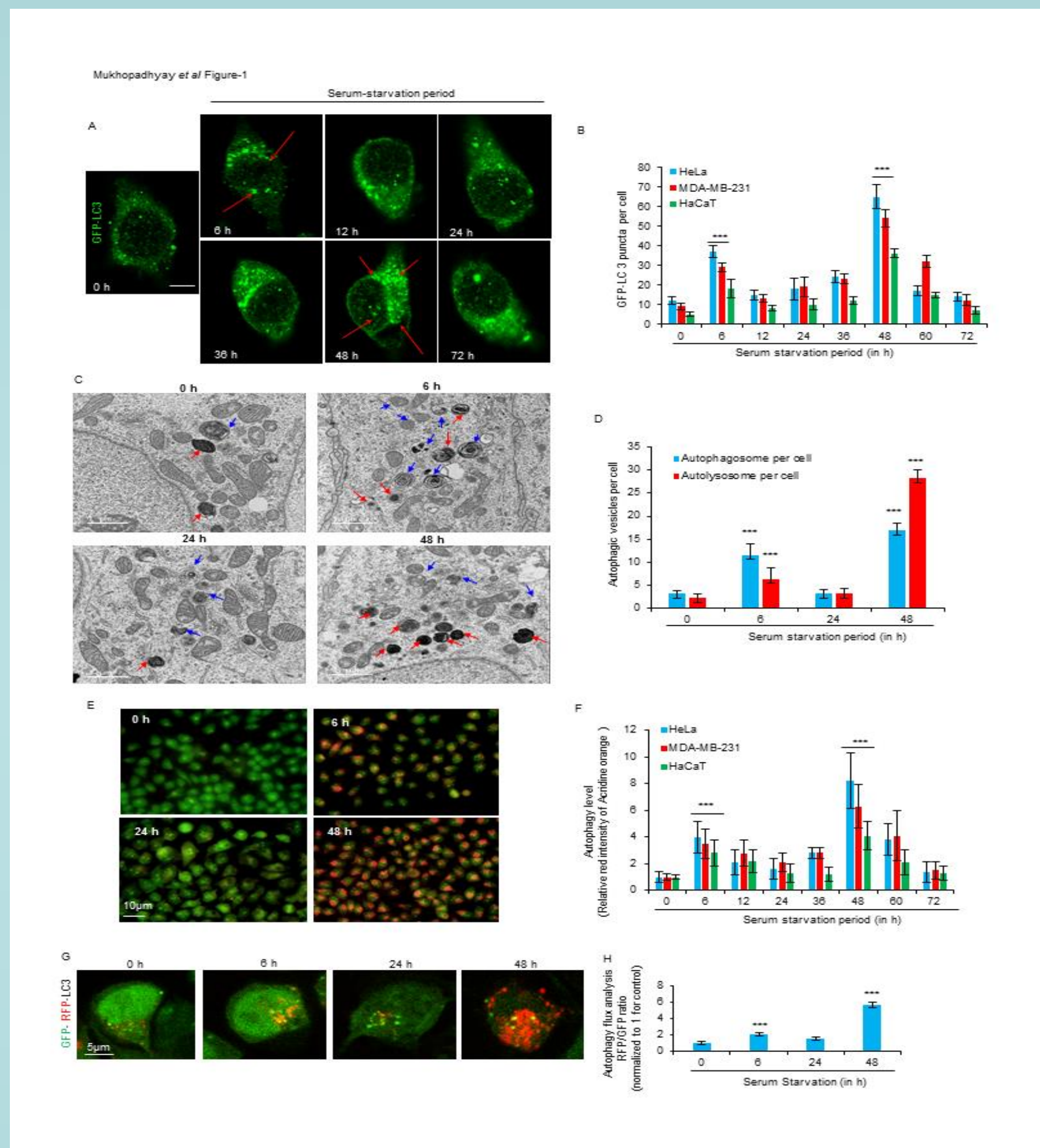


Figure 1: Serum starvation induces non-linear autophagy: (A) HeLa cells expressing GFP-LC3 were serum-starved for the indicated time period and examined by confocal microscopy. (B) LC3 puncta were enumerated in HeLa, MDA-MB-231 and HaCaT cells. Autophagosome formation was quantified, and data are presented as percentage of GFP-LC3-transfected cells with punctate fluorescence to autophagosome formation. A minimum of 100 GFP-LC3-transfected cells was counted. (C) HeLa cells were processed for transmission electron microscopy (blue arrow, autophagosome; red arrow, autolysosome) followed by quantification of autophagic vesicles (D). (E) Microscopic images of acridine orange stained HeLa cells in serum-starved conditions for the indicated periods were identified and stained for autophagic vesicles, relative red intensity was measured in HeLa, MDA-MB-231 and HaCaT cells (F). (G) Microscopic images of autophagic flux in GFP-RFP-LC3 plasmid expressing HeLa cells during serum starvation. Autophagy flux analysis was measured as RFP/GFP ratio (H). *** denotes $p < 0.001$ was considered statistically significant.

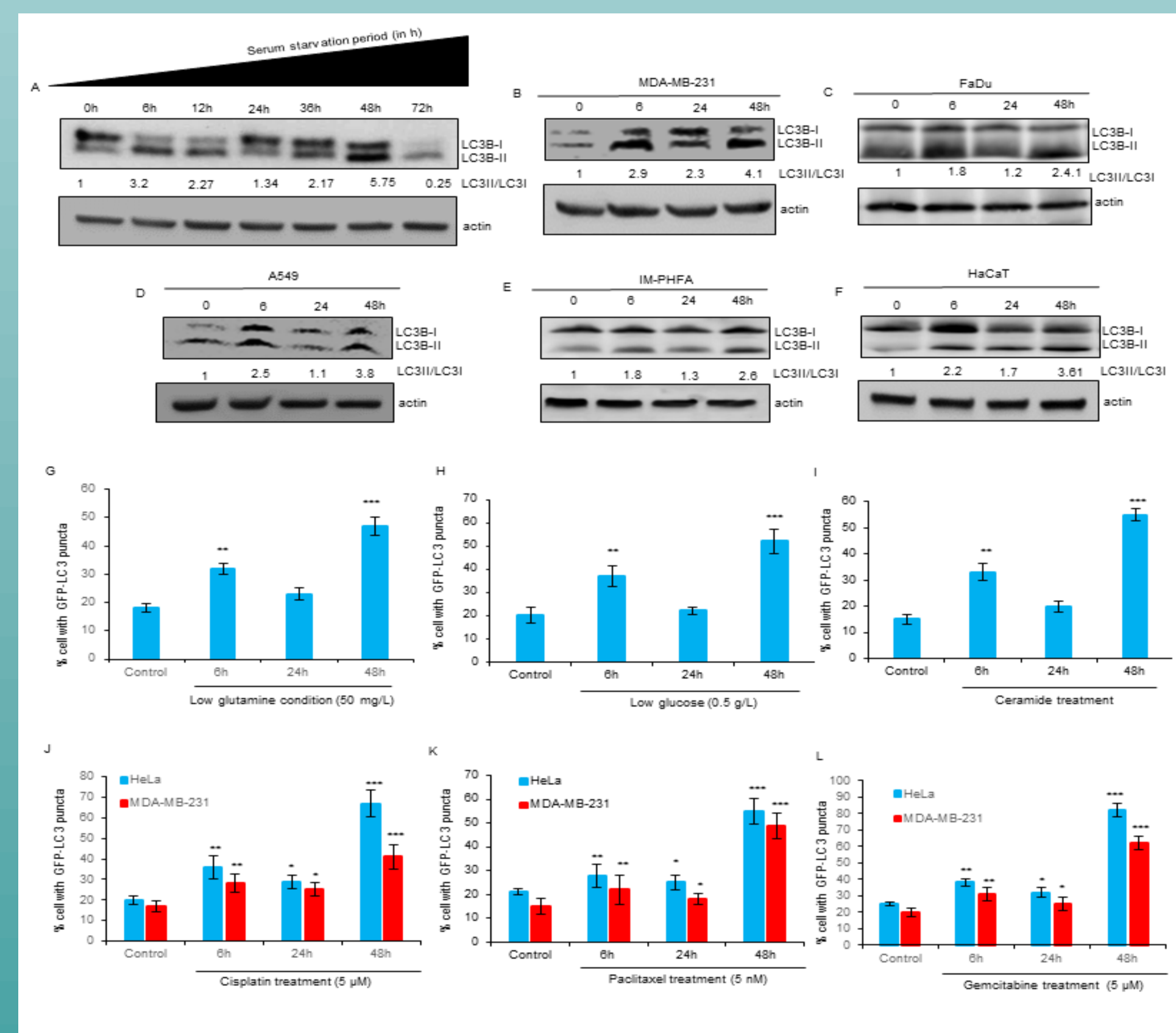


Figure 2: Autophagic oscillations in response to different stresses: Cell lysates of cancerous (A: HeLa, B: MDA-MB-231, C: FaDu, D: A459) and normal (E: IM-PHFA, F: HaCaT) cells following the indicated periods of serum starvation were probed for the level of LC3 accumulation. HeLa cells were incubated in DMEM lacking sufficient quantities of important metabolites – low glutamine (50 mg/L), low glucose (0.5 g/L) conditions and induced GFP-LC3 expression in HeLa cells was quantified (G), (H), respectively. (I) Ceramide treatment was done in HeLa cells expressing GFP-LC3 to quantify the autophagic puncta over the indicated periods. Clinically used chemotherapeutic agents including cisplatin (5 μ M) (J), paclitaxel (5 nM) (K), and gemcitabine (5 μ M) (L) were used on GFP-LC3 expressing HeLa and MDA-MB-231 cells to analyze the autophagy roller coaster variation during the indicated time points. LC3-II/I values are indicated after densitometric analysis. The p value was defined as follows: *; $p < 0.05$; **; $p < 0.01$; ***; $p < 0.001$ were considered statistically significant.

2. Irreversible autophagic progression beyond a point of no return leads to autophagy-dependent cell death

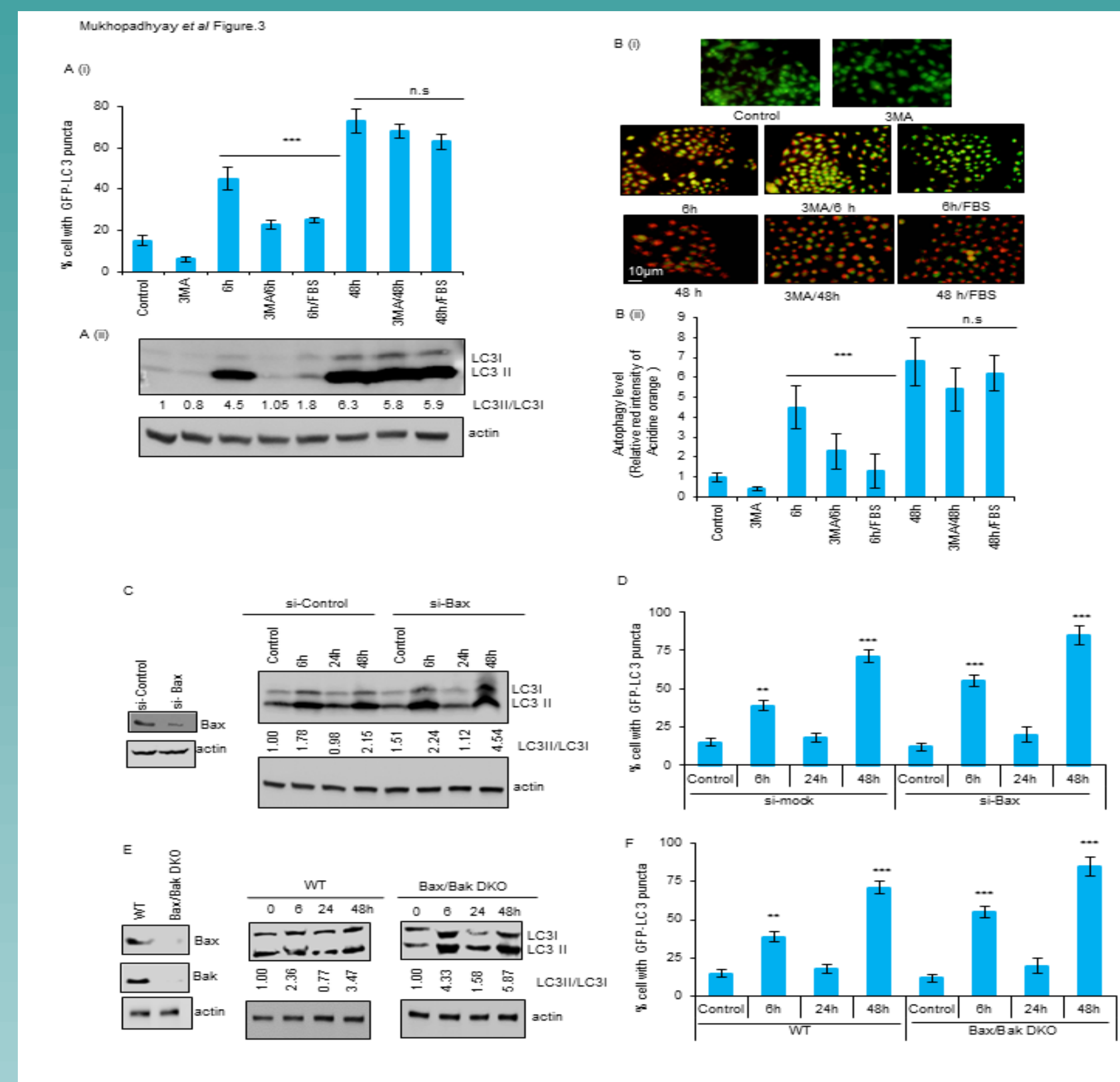


Figure 3: Deciphering the elusive "autophagic point of no return": (A) After serum starvation for the indicated periods, HeLa cells were incubated with 3-MA and FBS was reintroduced to prevent autophagy followed by analysis of autophagy through GFP-LC3 puncta formation by confocal microscopy (A.i), LC3 II accumulation by Western blotting (A.ii) and autophagic vesicle quantification by acridine orange staining (B.i, ii). HeLa cells were transfected with siBax and autophagy quantification was performed by LC3 II accumulation through Western blotting (C) and GFP-LC3 puncta formation by confocal microscopy (D). Similarly, Western blotting for LC3 expression (E) and GFP-LC3 puncta counting (F) was analyzed in serum-starved Bax/Bak double knock out (DKO) murine embryonic fibroblasts (MEFs). LC3-II/I values are indicated following densitometric analysis. The p value was defined as follows: not significant (n.s.); $p > 0.05$; *; $p < 0.05$; **; $p < 0.01$; ***; $p < 0.001$ were considered statistically significant.

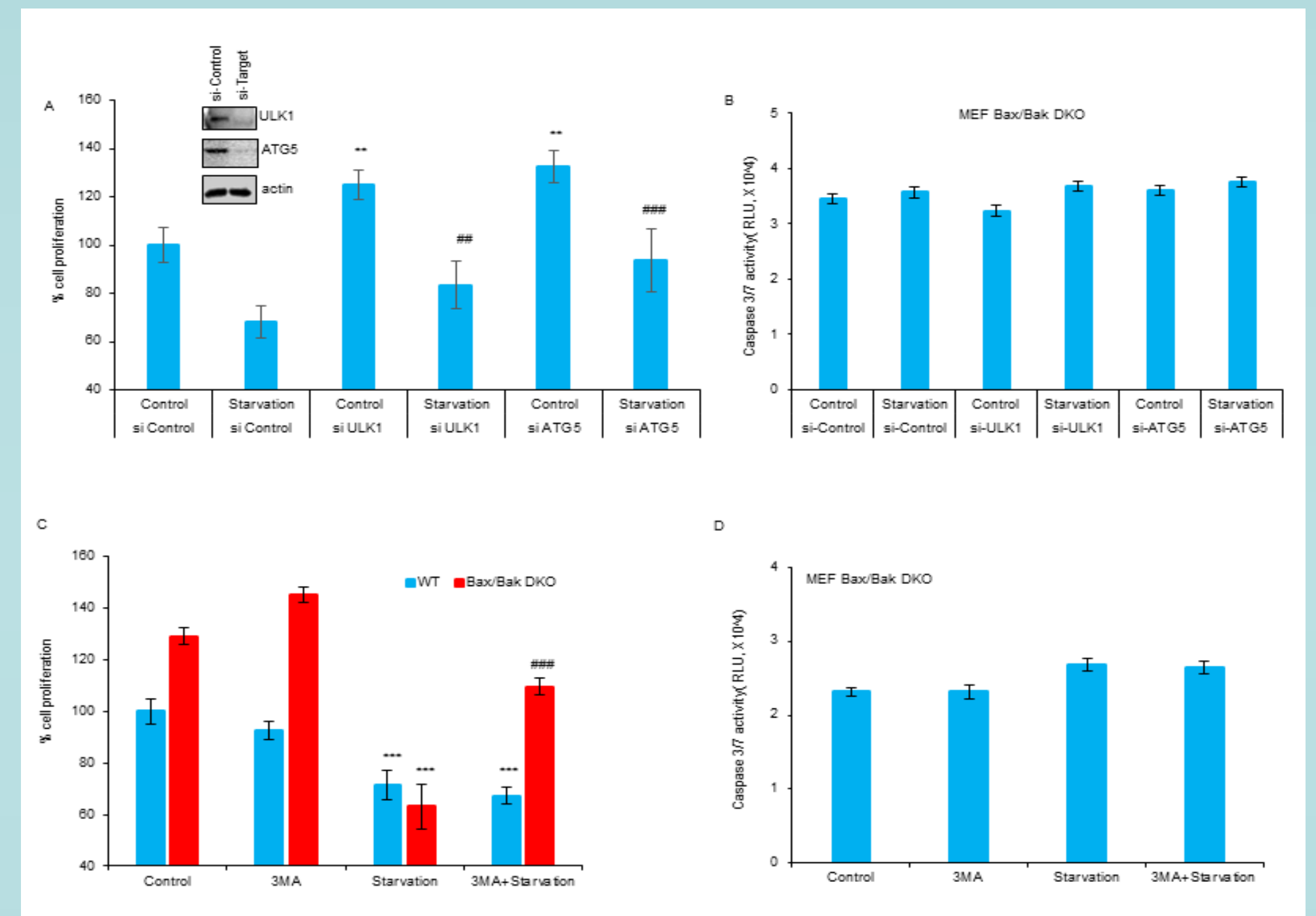


Figure 4: Autophagic cell death after point of no return in response to prolonged serum starvation. (A) The DKO MEFs were transfected with Ulk1 and ATG5 siRNAs and cell proliferation was determined by MTT assay (A) and caspase 3/7 activity by Caspase Glo assay (B) were quantified after 72 h of serum starvation (B). The DKO MEFs were pretreated with 3-MA to inhibit autophagy and cell proliferation (C) and caspase 3/7 levels (D) were determined after 72h of serum starvation. The p value was defined as follows: *; $p < 0.05$; **; $p < 0.01$; ***; $p < 0.001$ were considered statistically significant when compared with control under complete nutrient conditions while #; $p < 0.01$; ##; $p < 0.001$ were considered statistically significant when compared with control under serum starvation conditions.

3. mTOR controls autophagy fluctuation

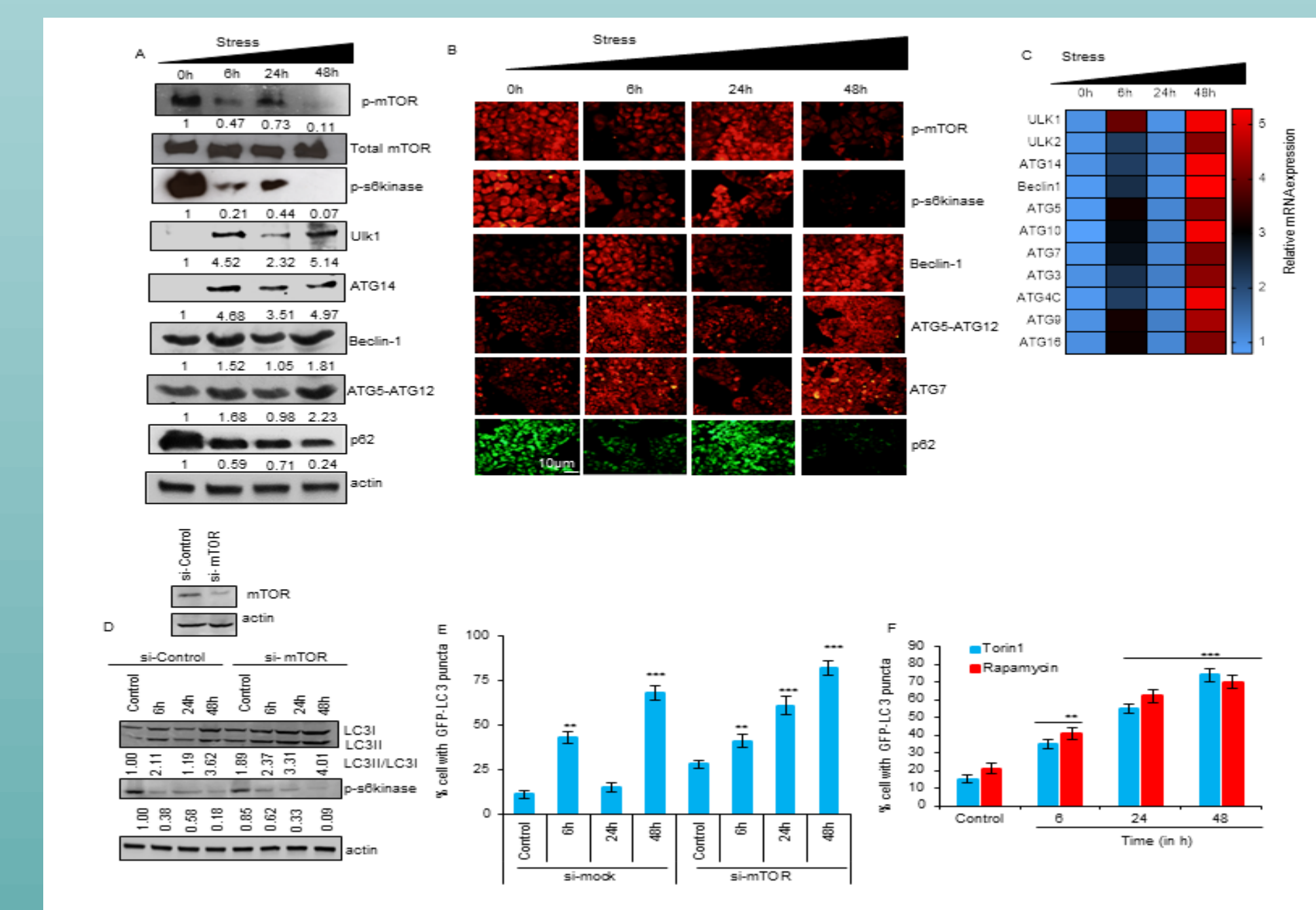


Figure 5: mTOR regulates the roller coaster variation during autophagy: After serum starvation for the indicated periods, the expression of key autophagic molecules was analyzed in HeLa cells at protein level by Western blotting (A) immunofluorescence analyses (B) and RNA level (C). mTOR was genetically knocked down in HeLa cells and LC3 expression was monitored by Western blotting (D) and GFP-LC3 puncta formation was determined microscopically (E) after serum starvation for the indicated times. LC3-II/I values are indicated as determined by densitometric analyses. (F) GFP-LC3 expressing HeLa cells were treated with Torin1 (200 nM) or Rapamycin (10 nM) for the indicated times and analyzed for GFP-LC3 puncta formation. ***; $p < 0.01$; ****; $p < 0.001$ were considered statistically significant when compared with controls.

4. Unbiased proteome-based screening strategy identifies Annexin A2 as an important modulator of autophagic fluctuation

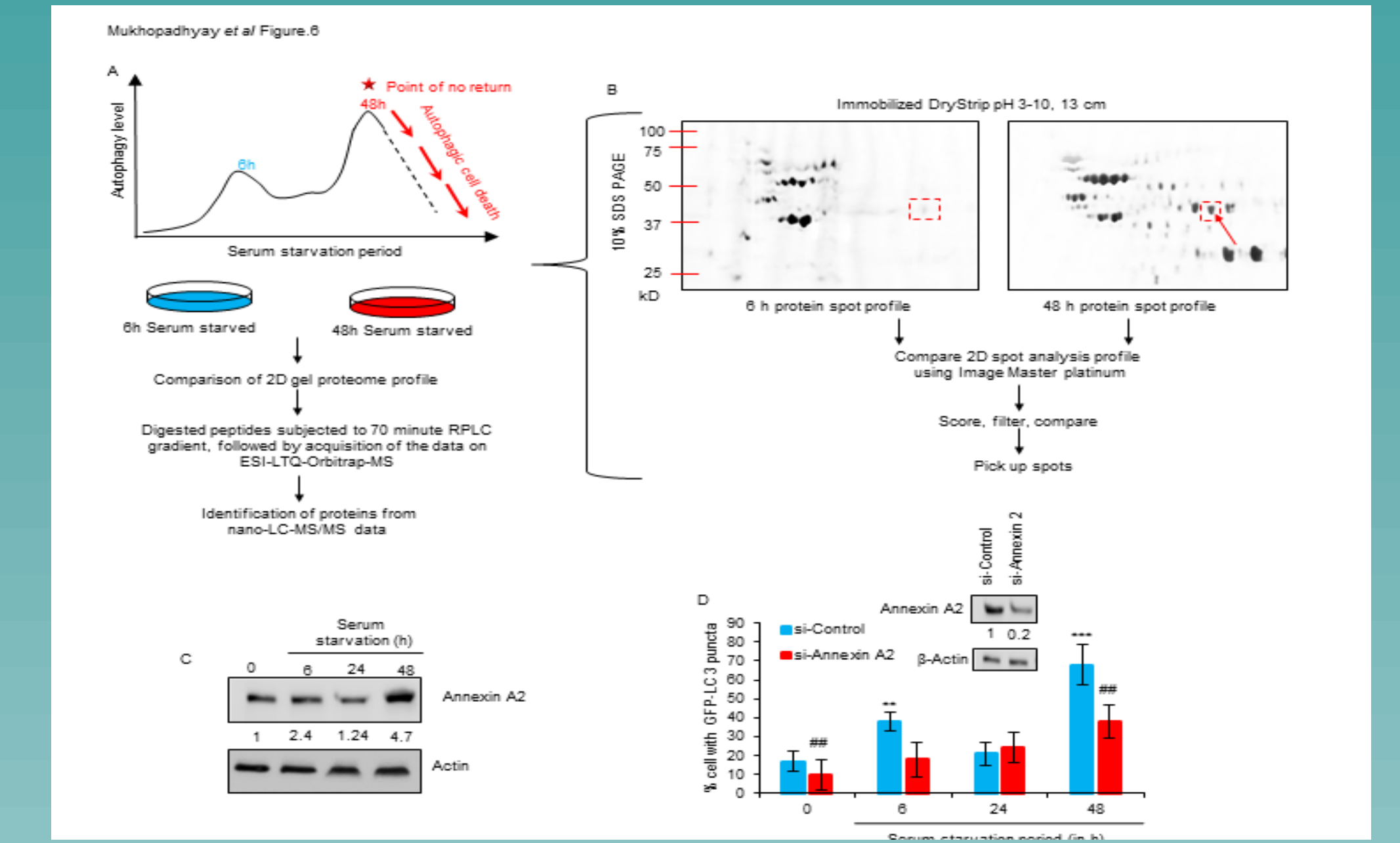


Figure 6: Proteomics analysis of the autophagic point of no return: (A) The pathway of workflow for proteomics analysis. (B) Two-dimensional gel electrophoresis (2DGE) after silver staining using HeLa cell lysates from serum-starved conditions for the indicated periods, indicating protein spots for mass spectrometric analysis, marked in the red box is Annexin A2. The 2DGE/LC-MS/MS data was validated for Annexin A2 by Western blotting (C) and the level of GFP-LC3 puncta was quantified (D) after knocking down Annexin A2 in GFP-LC3 expressing HeLa cells that were serum-starved for different times. **; $p < 0.01$; ***; $p < 0.001$ were considered statistically significant when compared with si-control under complete nutrient conditions.

5. Annexin A2 and mTOR interactions regulate autophagic fluctuations

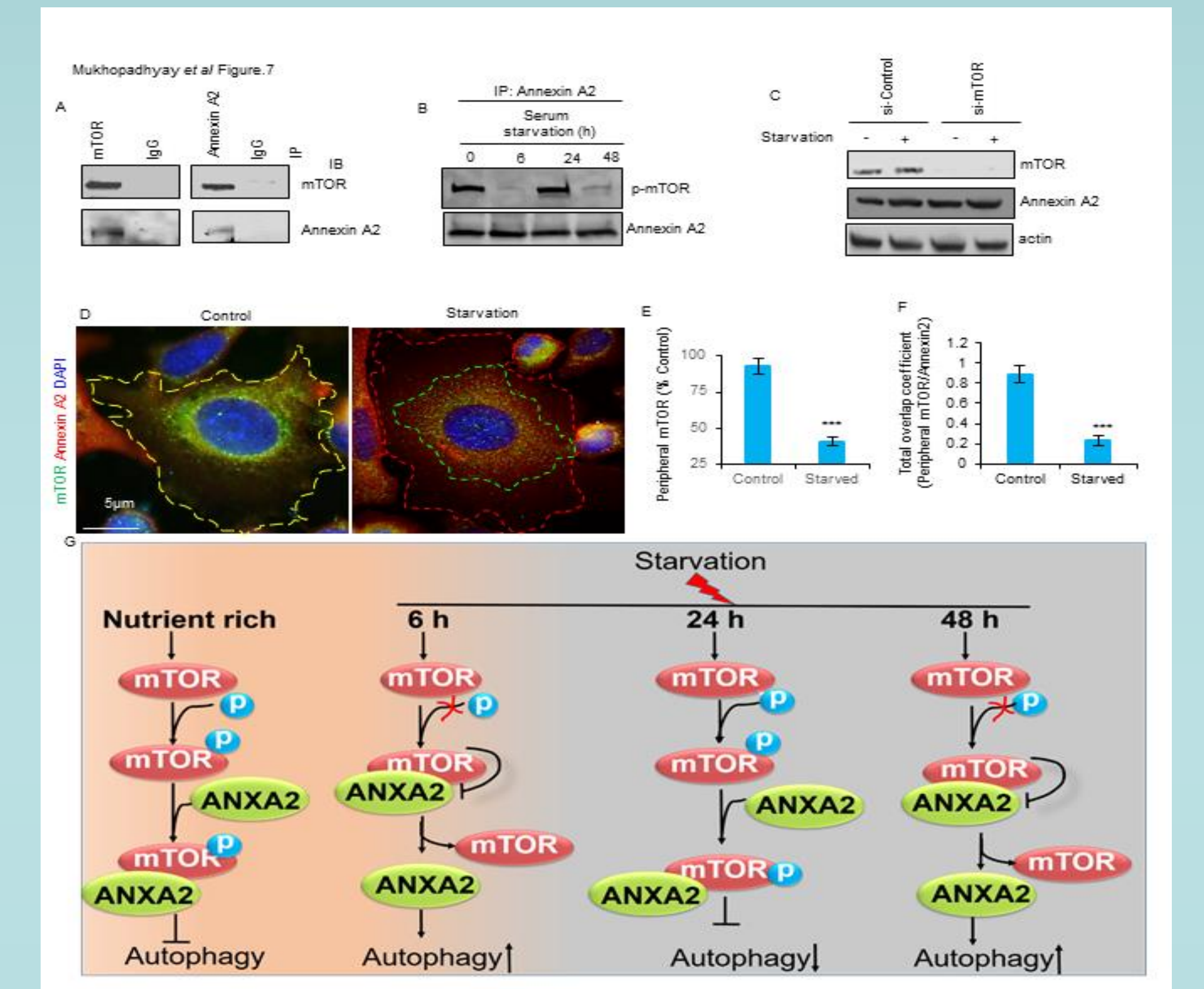


Figure 7: Annexin A2 and mTOR dynamically regulate oscillatory autophagic fluctuations: (A) HeLa cell lysates were immunoprecipitated with anti-mTOR and anti-Annexin A2 followed by immunoblotting with anti-Annexin A2 or anti-mTOR antibodies. (B) Annexin A2 was immunoprecipitated from HeLa cells grown for the indicated periods under serum starvation conditions and were analyzed for the active form of phosphorylated mTOR. (C) HeLa cells were transfected with si-mTOR and expression of Annexin A2 was determined by Western blotting. (D) Confocal microscopic analysis of spatiotemporal localization of mTOR and Annexin A2 was performed in HeLa cell controls and 6 h serum-starved conditions; followed by peripheral mTOR imaging (E), total overlap coefficient (between peripheral mTOR and Annexin A2) analysis (F) using ImageJ. The external boundary of control cell was marked by yellow dotted line marking peripheral overlap between Annexin A2-mTOR. The external boundary of the 6 h starved cell was marked by red dotted line with Annexin A2 and green dotted line indicated the region beyond which mTOR was dispersed.***; $p < 0.001$ was considered statistically significant when compared with control. (G) Schematic model illustrating the possible molecular mechanism of roller coaster form of non-linear autophagy during stress.

CONCLUSION

In summary, the present study provides insights into the process of nonlinear autophagic fluctuation that can lead to irreversible autophagic progression beyond the point of no return, which culminates in autophagy-dependent cell death in response to stress. Moreover, we identify mTOR as a unique regulator of Annexin A2 in the roller coaster model of autophagic fluctuation.

ACKNOWLEDGEMENT

We thank National Institute of Technology, Rourkela for providing a facility for this research work. Research support was partly provided by Department of Biotechnology [Grant Number: BT/PR7791/BRB/10/1187/2013 to SKB]. Centre for Cellular And Molecular Platforms (C-CAMP) is acknowledged for proteomics analysis.